

1967

The construction of a vibrating plate shearometer to determine the shear modulus of viscoelastic fluids

Richard Arnold Eelman
Lehigh University

Follow this and additional works at: <https://preserve.lehigh.edu/etd>

 Part of the [Chemical Engineering Commons](#)

Recommended Citation

Eelman, Richard Arnold, "The construction of a vibrating plate shearometer to determine the shear modulus of viscoelastic fluids" (1967). *Theses and Dissertations*. 5063.
<https://preserve.lehigh.edu/etd/5063>

This Thesis is brought to you for free and open access by Lehigh Preserve. It has been accepted for inclusion in Theses and Dissertations by an authorized administrator of Lehigh Preserve. For more information, please contact preserve@lehigh.edu.

THE CONSTRUCTION OF A VIBRATING PLATE SHEAROMETER TO
DETERMINE THE SHEAR MODULUS OF VISCOELASTIC FLUIDS

by

Richard Arnold Eelman

A Research Report
Presented To The Graduate Faculty Of
Lehigh University
In Candidacy For The Degree Of
Master Of Science

Lehigh University
Department Of Chemical Engineering
Bethlehem, Pennsylvania
1967

Certification Of Approval

This thesis is accepted and approved in partial fulfillment of the requirements for the degree of Master of Science.

1 August 1967
Date

Gary Poehlein
Professor in Charge

Head of the Department

Acknowledgements

The author is grateful to Prof. G.W. Poehlein and Mr. W.D. Schaeffer for their assistance in completing this work. Also, acknowledgements are due Messrs. L.J. Davis and J. Hosiak for their assistance in the construction of the instrument. The project was supported by the National Printing Ink Research Institute.

Contents

	Page
Abstract	1
Introduction	2
Theory	4
Design	13
Procedure	21
Results and Discussion	23
Conclusions	39
Recommendations for Future Work	42
Appendix	
A-Equipment Specifications	43
B-Data	45
C-Discussion of Microvoltmeter	47
References	48
Vita	50

Figure	<u>Figures</u>	Page
1. Shear modulus as a function of time for different materials.		4
2. Shear deformation of a body.		5
3. Stress and strain curves of a viscoelastic fluid subjected to sinusoidal shear deformation as viewed from a stationary position.		6

Figure	Page
4. Vector representation of complex shear modulus.	7
5. Sinusoidal shear wave propagated uni-dimensionally in a fluid.	8
6. Determination of the wave length.	11
7. Photograph of the shearometer.	14
8. Drawing of the shearometer.	15
9. Illustration of linear strain.	17
10. Schematic diagram of shearometer.	19
11a Sample calculation.	21
11b Sample calculation.	22
12. Elastic modulus versus frequency, H-50.	24
13. Viscous modulus versus frequency, H-50.	25
14. Elastic modulus versus frequency, 4% dispersion.	26
15. Viscous modulus versus frequency, 4% dispersion.	27
16. Elastic modulus versus frequency, 8% dispersion.	28
17. Viscous modulus versus frequency, 8% dispersion.	29
18. Elastic modulus versus frequency, comparison of three systems.	30
19. Viscous modulus versus frequency, comparison of three systems.	31
20. Time-domain shear modulus, H-50 and 4% dispersion.	32
21. Extrapolation of dynamic viscosity versus frequency to $\log f = 0$.	37
22. Linear response of transducer.	38

Figure	Page
23. Amplifier circuit diagram.	44
Table	
1. Key to Figure 8.	16

Abstract

A shearometer has been constructed for use in determining the complex shear modulus of viscoelastic fluids.

A sinusoidal shear wave is propagated between two parallel plates immersed in a viscoelastic fluid. The wave length and damping factor of the wave are determined from measurements of the stress exerted on the plates by the oscillating fluid. The wave length and damping factor are used to calculate the complex shear modulus of the fluid. The instrument will operate over the frequency range, 100cps to 10 Kc.

Experimental testing was done on dispersion systems of carbon black in polybutene. The dynamic viscosity as determined by the shearometer for an 8% by weight dispersion was 150 poise. The viscosity as determined by a rotational viscometer was 190 poise. The two agree within the experimental accuracy of the instrument. The complex shear modulus was also calculated for the dispersion systems.

Results of the testing indicate that the shearometer is an accurate and convenient way to obtain shear modulus data for viscoelastic fluids.

Introduction

The stress-strain relationship for viscoelastic fluids must be characterized if flow behavior is to be described. Viscoelastic fluids which may be represented by simple models as described in Ferry (1) have stress-strain relationships which can be characterized by a time dependent shear modulus or a frequency dependent complex modulus. The frequency dependent complex modulus is the Fourier transform of the time dependent shear modulus.

Several methods (2,3,4) are described in the literature for determining the complex shear modulus but most are limited in the frequency range over which measurements can be made.

Miles(5) and Miller, et al(6) have developed instruments capable of determining the shear modulus over a wide frequency range but these methods are limited to very high viscosity fluids.

Ferry(1) describes a method for determining the complex shear modulus by measuring the wave length and damping of a sinusoidal shear wave propagated in a viscoelastic fluid. The measurement of the parameters is based on the birefringence of the fluid when strained. The

method is limited to transparent fluids.

The design of the instrument described in this report was based on the theory developed by Ferry(1) but uses different measuring techniques.

Theory

The shear modulus for linear viscoelastic fluids is defined by the relationship,

$$(1) G(t) \equiv \tau(t)/\gamma$$

where: $\tau(t)$ = stress varying with time

γ = strain applied at $t = 0$.

Linear viscoelastic behavior exists when the ratio of stress to strain is a function of time only and not a function of the stress magnitude. For example, in an elastic solid such as steel, linear behavior exists only below the elastic limit. If the elastic limit is exceeded, the stress-strain ratio depends on the stress magnitude as well as time.

$G(t)$ is constant for a perfect elastic material as shown in Figure 1a.

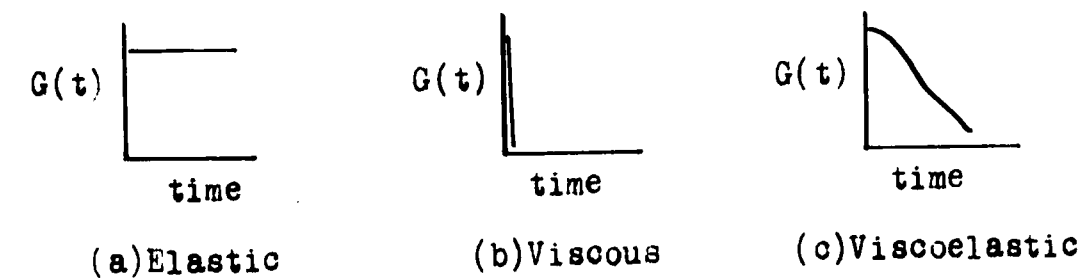


Figure 1-Shear modulus as a function of time for different materials

If the perfect elastic body shown in Figure 1a is

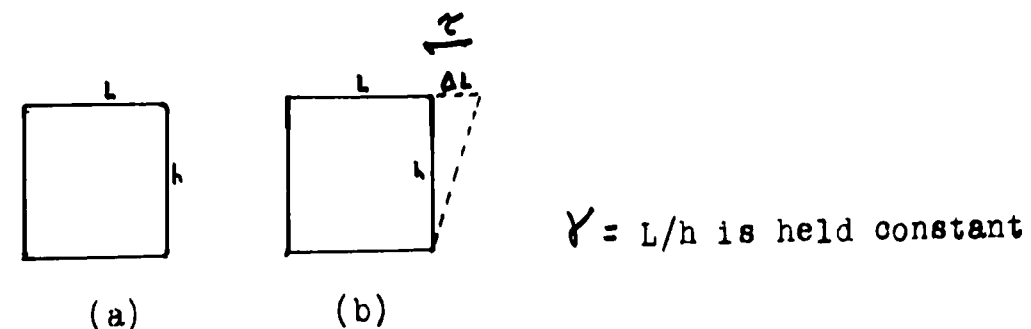


Figure 2-Shear deformation of a body.

subjected to a shear strain $\Delta L/h$ (Figure 2b) a stress τ develops equal to the stress necessary to deform the body. This stress will remain as long as the strain is held. Therefore $G(t)$ is constant with time.

$G(t)$ for a perfect viscous fluid is a Dirac impulse function at $t=0$ since τ is a function of rate of strain rather than strain. If the body in Figure 2 were a perfect viscous body and were subjected to an instantaneous strain of the amount $\Delta L/h$, the stress associated with the strain would immediately go to zero and $G(t)$ would appear as shown in Figure 1b.

$G(t)$ for a viscoelastic fluid falls between the two limiting cases described above (Figure 1c) depending on the particular properties of the fluid.

If the body described in Figure 2 were viscoelastic and were subjected to the instantaneous strain, $\gamma = \Delta L/h$ as shown in Figure 2b, $G(t)$ could be determined directly if τ could be measured as a function of time. This method of

determining $G(t)$ is impractical for most viscoelastic fluids since $\gamma(t)$ decays to zero so rapidly that it is not possible to measure force as a function of time.

If a viscoelastic fluid experiences a sinusoidal shear deformation, a steady state situation develops in which stress and strain become functions of the frequency of deformation. The stress lags the strain by a constant angle ϕ and both vary sinusoidally having the same period. The complex shear

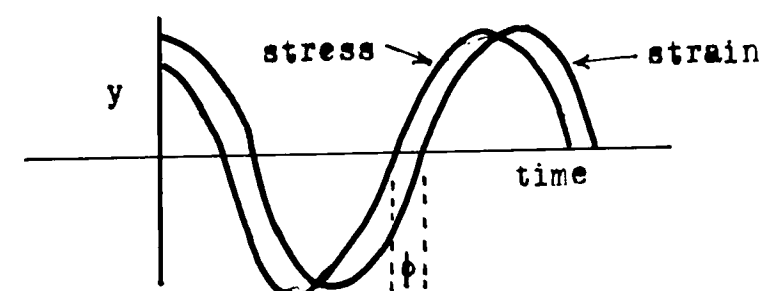


Figure 3- Stress and strain curves of a viscoelastic fluid subjected to sinusoidal shear deformation as viewed from a stationary position.

modulus, $G^*(\omega)$, is defined as a vector quantity, the magnitude of which is the ratio of peak stress to peak strain and the direction of which is determined by the angle ϕ defined above. The vector is a function of the frequency of strain and is composed of a real and an imaginary part as shown in Figure 4. The real part of the complex shear modulus, $G'(\omega)$, represents the component of the stress in phase with the strain or the elastic component of the complex shear

modulus. The imaginary part, $G''(\omega)$, represents the component of the stress 90° out of phase with the strain or the viscous component of the complex modulus. The time dependent shear modulus, $G(t)$, can be related to $G''(\omega)$ through the inverse Fourier transforms:

$$(2) \quad G(t) = \frac{2}{\pi} \int_0^\infty (G'(\omega)/\omega) \sin \omega t \, d\omega$$

$$(3) \quad G(t) = \frac{2}{\pi} \int_0^\infty (G''(\omega)/\omega) \cos \omega t \, d\omega$$

Hence, if $G'(\omega)$ or $G''(\omega)$ are known over a relatively wide frequency range, $G(t)$ may be obtained by numerical integration of the above equations.

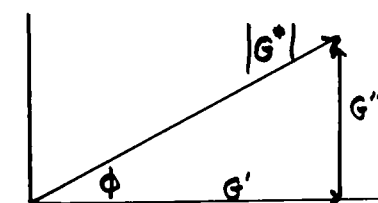


Figure 4-Vector representation of complex shear modulus.

The components of the complex shear modulus can be calculated directly from a knowledge of the complex modulus vector $G^*(\omega)$ and the associated phase angle ϕ . However, calculation of $G^*(\omega)$ or ϕ requires a characterization of the shear wave propagated by the sinusoidal shear deformation of the fluid. Equation 4, given by Ferry(1), is the

$$(4) u = u_0 \exp(i(\omega t - 2\pi x/\lambda) - x/x_0)$$

where: u = displacement of fluid in z direction.

u_0 = peak displacement at $x = 0$.

λ = wave length of shear wave.

x_0 = critical damping distance, i.e. value of x where $u = u_0/e$

mathematical representation of a sinusoidal shear wave propagated in a fluid of infinite extent and approximating a one dimensional disturbance as shown in Figure 5.

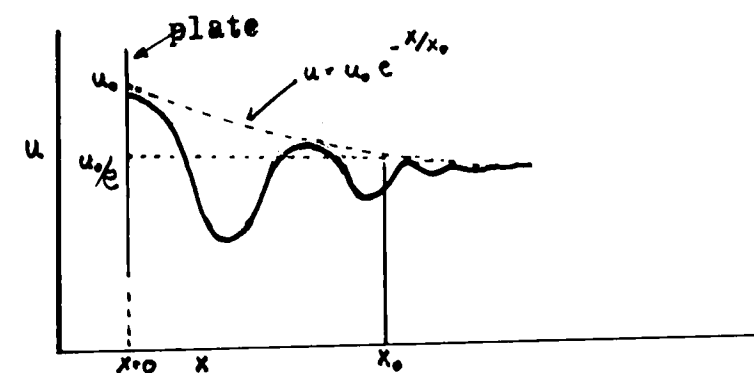


Figure 5-Sinusoidal shear wave propagated uni-dimensionally in a fluid.

The wave equation applicable here is

$$(5) \nabla^2 u + \beta^2 u = 0$$

$$(6) \beta = [\beta_1 - i\beta_2] = \left\{ \frac{\rho \omega^2}{G' + iG''} \right\}^{1/2}$$

where: ρ = density of the medium

$$\beta_1 = 2\pi/\lambda$$

$$\beta_2 = 1/x_0$$

Therefore,

$$(7) \quad G'(\omega) = \frac{\omega^2 \lambda^2 \rho [4\pi^2 - (\lambda/x_0)^2]}{[4\pi^2 + (\lambda/x_0)^2]^2}$$

$$\text{and } (8) \quad G''(\omega) = \frac{4\pi \omega^2 \lambda^2 \rho (\lambda/x_0)}{[4\pi^2 + (\lambda/x_0)^2]^2}$$

Hence, if λ and x_0 are known at a given frequency, $G'(\omega)$ and $G''(\omega)$ can be calculated at that frequency.

Adler, et al(7) have attacked the problem of a sinusoidal shear wave propagated in a finite medium. They solved the wave equation,

$$(5) \quad \nabla^2 u + \beta^2 u = 0$$

using the following boundary conditions,

1) $u(x, y) \rightarrow 0$ for large value of x .

2) $u(x, y) = 0$, where $2y_0$ is the y dimension of the medium.

3) $u(0, y) = \begin{cases} u_0 & \text{for } |y| \leq y_0 \\ 0 & \text{for } |y| > y_0 \end{cases}$, where $2y_0$ is the width of the plate generating the wave.

The solution obtained for Equation 5 using the above boundary conditions was,

$$(9) \quad u(x, y) = \frac{4}{\pi} u_0 \sum_{n=0}^{\infty} \frac{1}{2n+1} \exp(-\alpha_n x) \sin\left[(n+\frac{1}{2}) \frac{\pi y_0}{y_1}\right] \cos\left[(n+\frac{1}{2}) \frac{\pi y}{y_1}\right]$$

$$\text{where: } \alpha_n = \left[-\beta^2 + (n + \frac{1}{2})^2 (\pi^2 / 4) \right]^{1/2}$$

showing that the relationship between u and u_0 is not a simple exponential decay as indicated by Equation 4 for an infinite medium but rather a series of exponentials. However, if measurements are made at large distances from the driven plate, the values of x_0 and λ obtained from Equation 4 will yield good approximations to the true values since the second through n terms in Equation 9 will be negligible in comparison to the first.

Now,

$$(10) \quad G^*(\omega) \equiv \tau(\omega) / \gamma(\omega)$$

where G^* is the ratio of peak stress to peak strain.

and at a given frequency, $\gamma \propto u$ which defines the values of x_0 and λ . τ is the stress associated with the wave amplitude u and, $\tau \propto u$. Therefore,

$$(11) \quad \tau = \tau_0 \exp(i(\omega t - 2\pi x/\lambda) - x/x_0)$$

If the stress associated with the motion is known, x_0 and λ can be determined.

In the work reported here, the stress was measured by means of an electro-mechanical transducer so that stresses were measured in terms of voltages. The value, x_0 , was

obtained from the relationship,

$$(12) V = V_0 \exp(-x/x_0)$$

where: V is the voltage measured at x .

V_0 is the voltage corresponding to $x = 0$.

If the value of V is known at two different values of x , the relationship,

$$(13) \ln(V_2/V_1) = (x_1 - x_2)/x_0$$

is obtained and yields x_0 directly. The wave length, λ , is obtained from a measurement of the phase shift of the shear wave for a change in x through the relationship,

$$(14) \lambda = (x_1 - x_2)/(\phi/2\pi)$$

where: ϕ is the phase shift of the shear wave as shown in Figure 6.

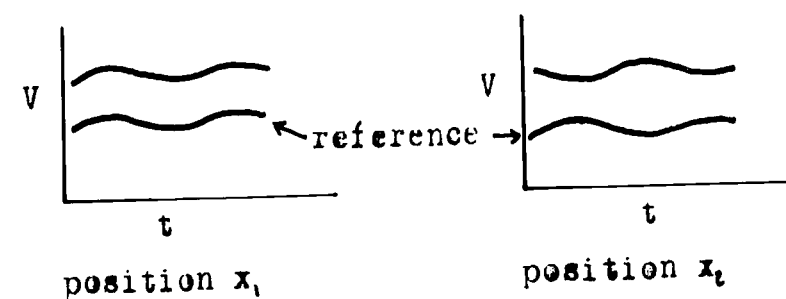


Figure 6-Determination of the wave length

At position x_1 , the shear wave is in phase with the reference wave while at position x_2 , the shear wave is 180° out of phase. Hence the wave length, λ , equals $(x_1 - x_2)/(\pi/2\pi)$ or $\lambda = 2(x_1 - x_2)$

The real and imaginary components of the complex shear modulus can be calculated using Equations 7 and 8.

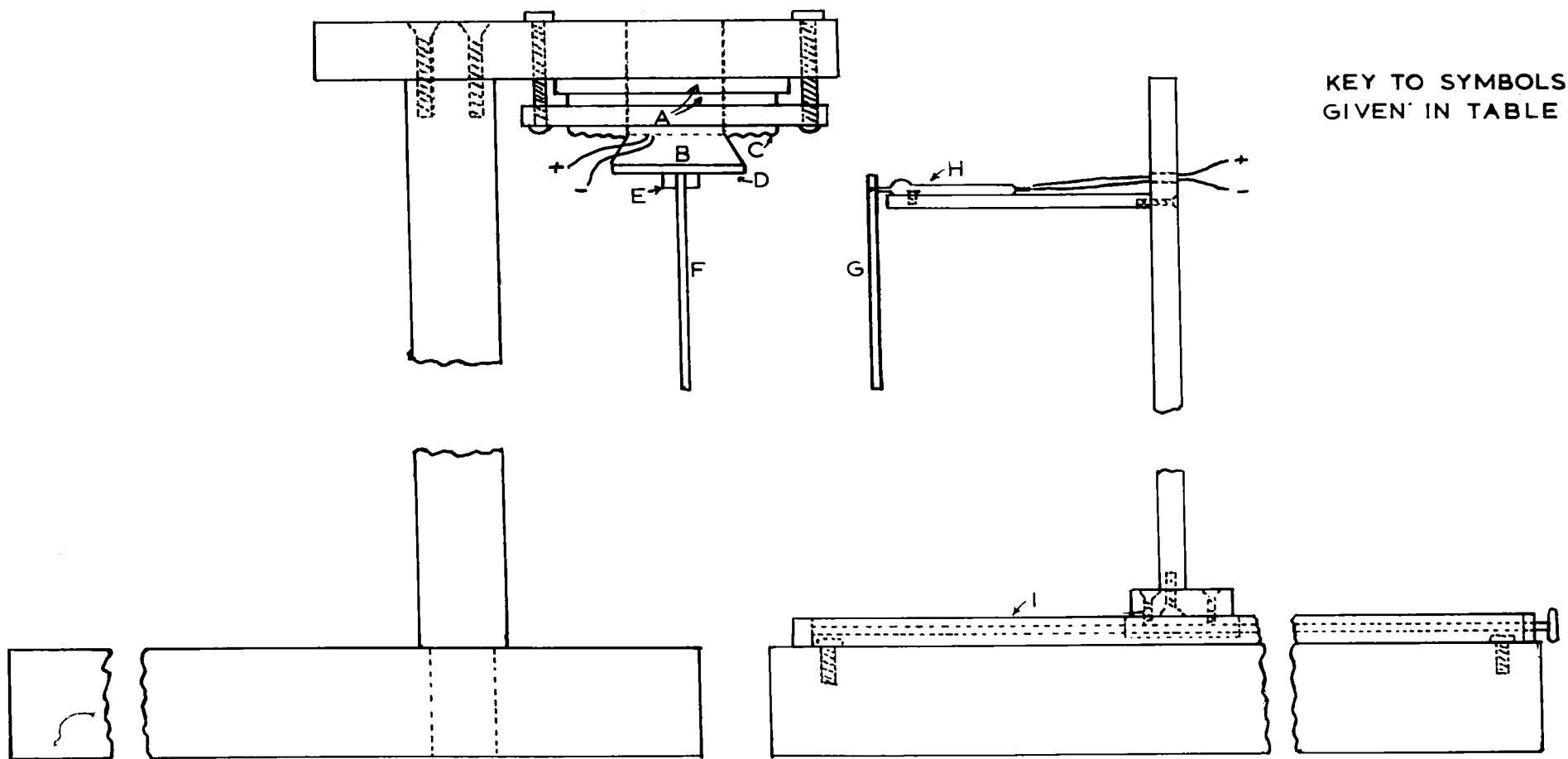
Design

The shearometer, shown in Figures 7 and 8, consists of two flat, parallel plates, the first of which is driven sinusoidally at a known frequency and the second of which responds to the stress associated with the propagated shear wave.

The design of the shearometer is a modification of similar instruments reported in the literature. Miles(5) and Miller, et al(6) describe instruments for measuring the complex shear modulus, $G^*(\omega)$, consisting of two parallel plates, one of which is driven sinusoidally and the other used to pick up the shear wave propagated in the liquid. The shearometer described here is similar to the instrument described by Miles with two exceptions: 1) the piezoelectric driver used by Miles is replaced by an electromagnetic driver so that the amplitude of the strain is increased, 2) the distance between the plates is generally much larger and can be varied. These differences were necessary because the method employed to measure $G^*(\omega)$ differs from that of Miles. The method developed by Miles requires that the plates be very close together so that the separation is only a small fraction of a wave length and the strain is linear as shown in Figure 9. Such operation would be questionable for low viscosity fluids in which the wave



FIGURE 7-SHEAROMETER



KEY TO SYMBOLS IS
GIVEN IN TABLE 1

FIGURE 8 - DESIGN OF SHEAROMETER

Table 1Key to symbols for Figure 8

A-Electromagnetic floating-coil speaker, Mustang m-12,
8 ohms.

B-Truncated section of speaker cone, 1 cm. in length.

C-Flexible diaphragm.

D-Lucite disk, $1/8$ in. thick by 3 in. diameter, bonded
to the cone.

E-Lucite blocks, $1/4$ in. square by $3/4$ in., supports
for plate.

F-Driver plate, $4-5/8$ in. by $3/4$ in. by $1/16$ in.
aluminum.

G-Pick-up plate, 4 in. by $3/4$ in by $1/16$ in. aluminum.

H- Pick-up transducer, Astatic No. 12 Phono-cartridge

I-Dovetail slide with vernier scale

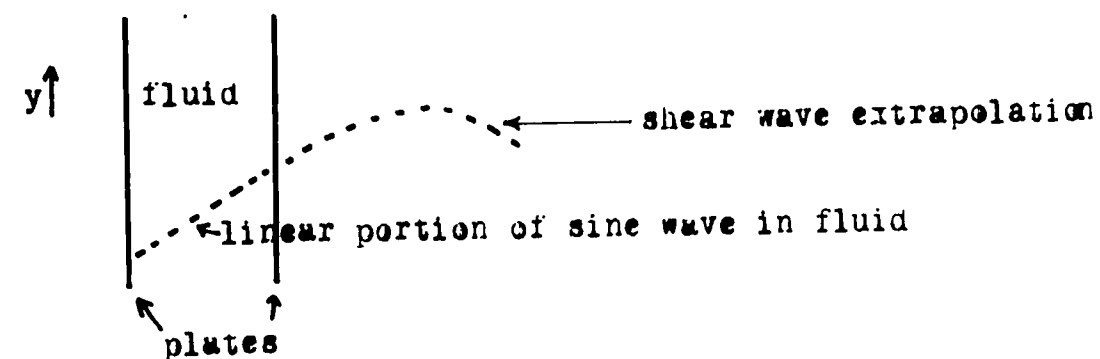


Figure 9-Illustration of linear strain.

is damped rapidly. Also, in the methods used by Miles and Miller the fluid had to remain between the plates, held there by capillary, viscous and adhesive forces. Low viscosity fluids could not be used in these systems.

The measurement of wave length and critical damping factor of a shear wave in the present instrument required relatively large separation of the plates. The amplitude of the strain had to be large so that the wave would provide a measurable stress at the distance involved. The motion of a piezoelectric driver is limited to about 10^{-4} cm. whereas an electromagnetic driver can generate motion of about 10^{-2} cm.

The design of the driver used in this work is similar to those described by Newman(8) and Smith, et al(4). The plate is a piece of 4-5/8 in. by 3/4 in. by 1/16 in aluminum and is driven by a modified floating-coil loudspeaker. (Equipment specifications are listed in Appendix B) The plate is bonded to the cone of the loudspeaker as shown in Figure 8.

The cone is held in place by a flexible diaphragm. The speaker cone is truncated leaving a one centimeter base to which the plate is mounted. The assembly is mounted in turn on an aluminum frame. The entire piece weighs about 45 lbs.

The pick-up plate is a piece of 4 in. by $3/4$ in. by $1/16$ in aluminum and is bonded to a piezoelectric phonograph transducer so that motion of the plate resulting from the applied stress affects the transducer in the same way a phonograph stylus does. The cartridge is bolted on a frame which rides on a dovetail slide equipped with a vernier scale capable of measuring to 0.001 in. The slide is bolted to a 20 lb. aluminum block.

The driver section of the instrument is separated from the pick-up section. Both pieces are separated from the bench on which they rest by foam rubber so that any vibrations which may occur in the driver section are damped out before they can be transmitted to the pick-up section by way of the bench. The transducer used in this instrument is extremely sensitive and therefore damping of external signals is critical to insure that any signal transmitted by the transducer comes only from the fluid. A small signal is picked up through the air, caused by sound waves propagated by the driver motion. These signals are negligible with respect to the signal transmitted through the fluid. The

entire instrument is grounded to eliminate stray electrical signals.

A schematic diagram of the shearometer and auxiliary equipment is shown in Figure 10. The loudspeaker is driven

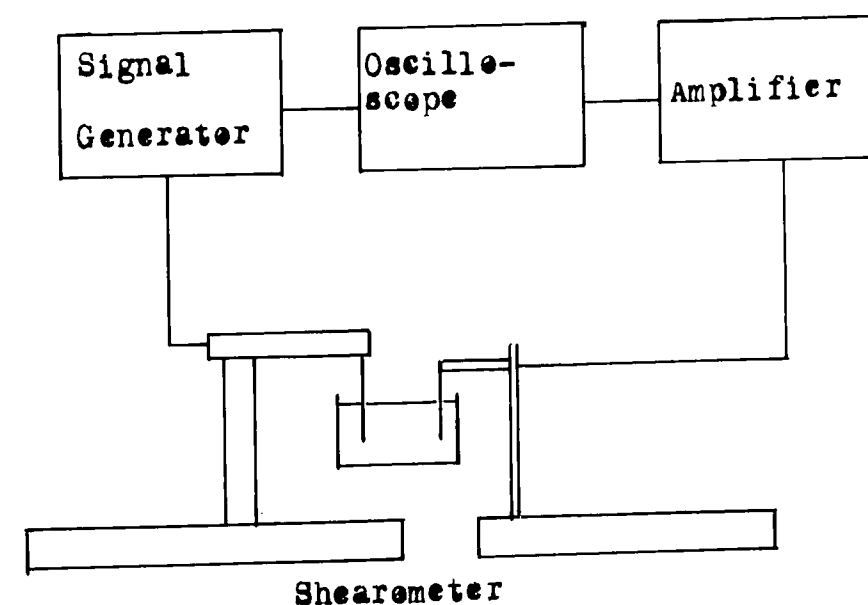


Figure 10-Schematic diagram of shearometer

by the one volt output from the signal generator. This low voltage is sufficient to drive the speaker within the frequency range studied. The signal from the signal generator is introduced into the upper beam of a dual beam oscilloscope and used as a reference signal. The signal coming from the cartridge is amplified by an R-C voltage amplifier with a gain of 1000 and also introduced into the oscilloscope. The amplifier circuit diagram is shown in

Figure 23, page 44. Some low frequency external vibrations were detected but the signal generated by them was filtered out with a tuned R-L-C circuit.

The fluid was held in a cylindrical container, 7 cm. in diameter and 9 cm. deep, into which the plates were immersed. The driver plate was centered in the container so that the distance between the driver plate and the pick-up plate was small compared to the distance between the driver plate and the wall of the container. The container was clamped to the bench top.

Procedure

The desired signal was introduced to the driver and monitored on the upper beam of the oscilloscope. The signal from the transducer was amplified and monitored on the lower beam of the oscilloscope. The position of the receiver plate on the slide was determined. The wave forms of the the generating and the received signals were photographed on the oscilloscope screen. The magnitude of the received signal and the phase angle between the two traces were determined from the photographs. The receiver plate was then moved to a different setting and the procedure repeated.

The voltages necessary to determine x_0 and the separations of the plates are measured directly. The difference in phase angles between the first and second plate separations must be determined to calculate λ . The phase angle shift and the plate separations are directly substituted into Equation 14. Sample calculations are shown below.

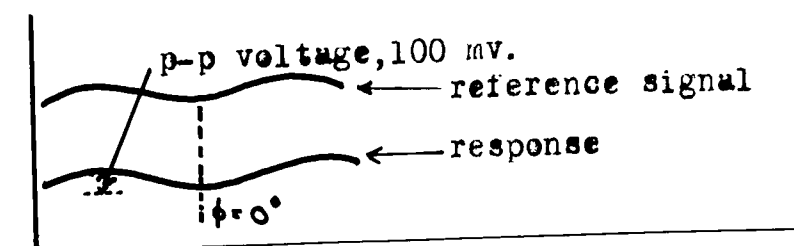


Figure 1Aa-Sample calculation, setting No. 1, $x_1 = 0.400$ in.

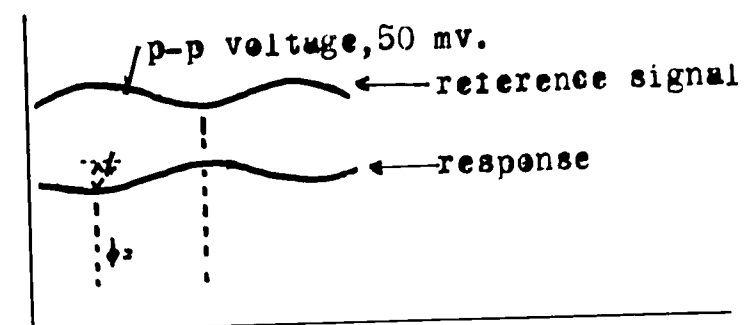


Figure 11b-Sample calculation, setting No. 2, $x_2 = 0.900$ in.

$$\ln(V_1/V_2) = (x_2 - x_1)/x_0$$

$$\ln(100./50.) = (0.900 - 0.400)/x_0$$

$$x_0 = 0.72 \text{ in.}$$

$$\lambda = (x_2 - x_1)/(\phi/2\pi)$$

$$\lambda = (0.500)/(\pi/2\pi)$$

$$\lambda = 1.00 \text{ in.}$$

Results and Discussion

Tests were made with a polybutene, H-50 and dispersions of carbon black in polybutene. The carbon black was "Elf-5", a medium flow channel black manufactured by the Cabot Corporation. "Elf-5" is non-porous and partially polar with a relatively narrow particle size, mean diameter being 257\AA . The apparent bulk density is 11.5 lbs./ft.

The vehicle, polybutene H-50, is a butylene polymer predominantly high molecular weight mono-olefins (85 to 98%), the balance being isoparaaffins. H-50 has an average molecular weight of 700, a viscosity at 25°C of 92.5 poise and a specific gravity of 0.878.

Three systems were studied, 100% H-50, 4% by weight "Elf-5" (2 % pigment volume concentration) in H-50 and 8% by weight "Elf-5" (4 % pigment volume concentration) in H-50. The carbon black was dried at 120°C for 12 hrs. before being added to the polybutene. The mixture was milled on a three-roll mill to a grindometer (9) reading of zero. Shear stress - shear rate properties of similar systems have been studied by Fischhoff(10).

The results of the tests are illustrated in Figures 12 to 20. Measurements were made two hours after the dispersions

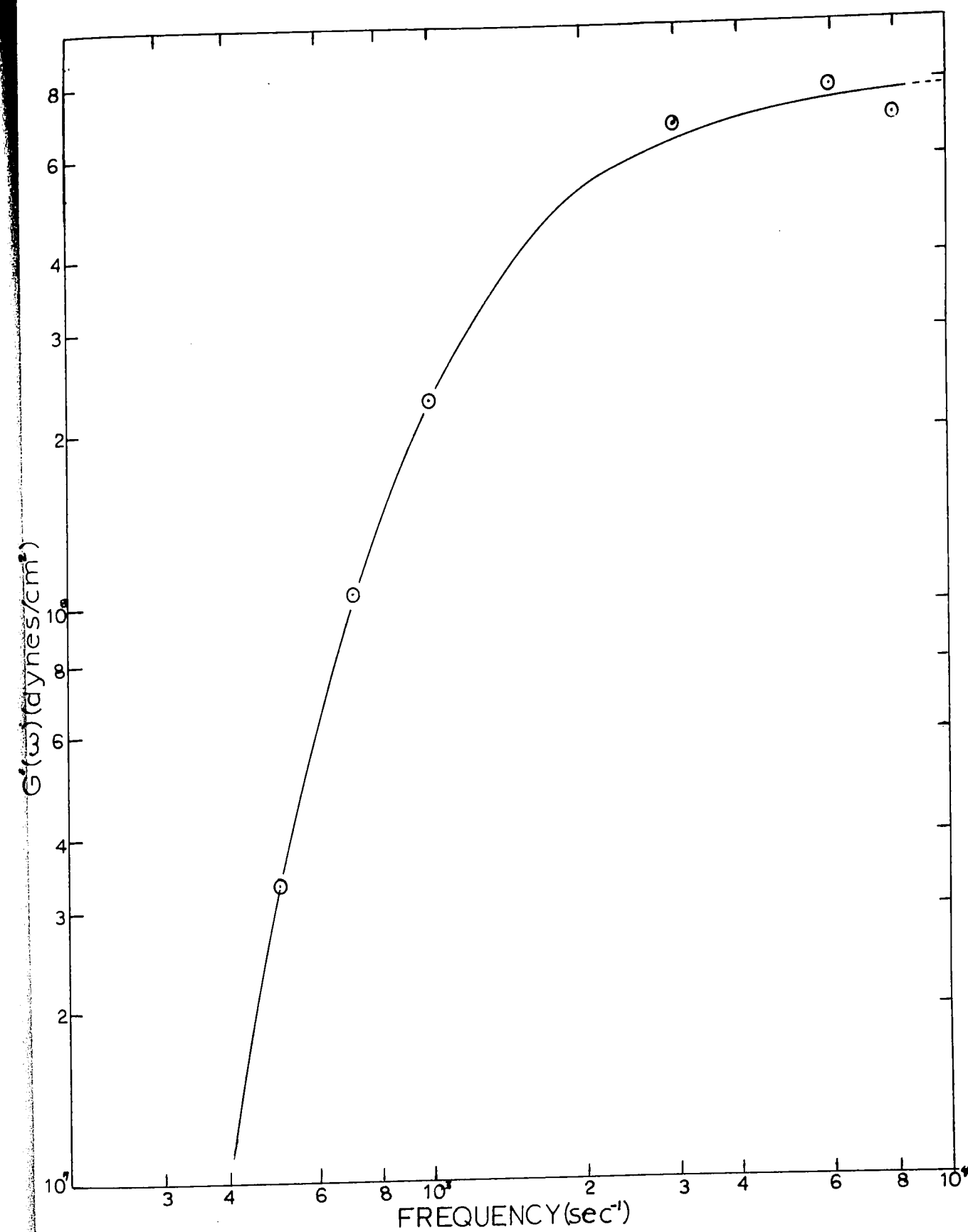


FIGURE 12- ELASTIC MODULUS VERSUS FREQUENCY FOR
PURE POLYBUTENE

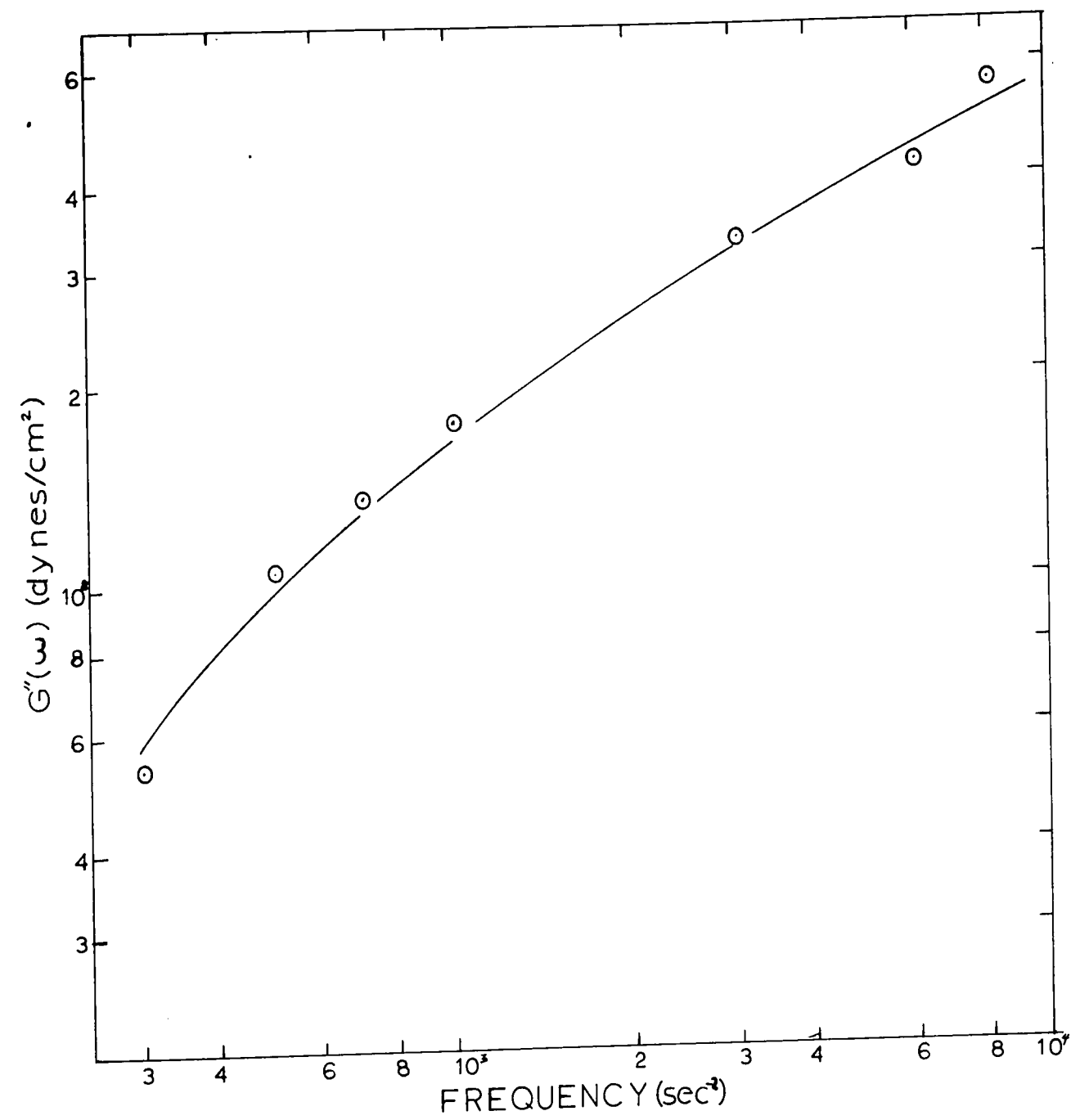


FIGURE 13- VISCOUS MODULUS VERSUS FREQUENCY
FOR PURE POLYBUTENE

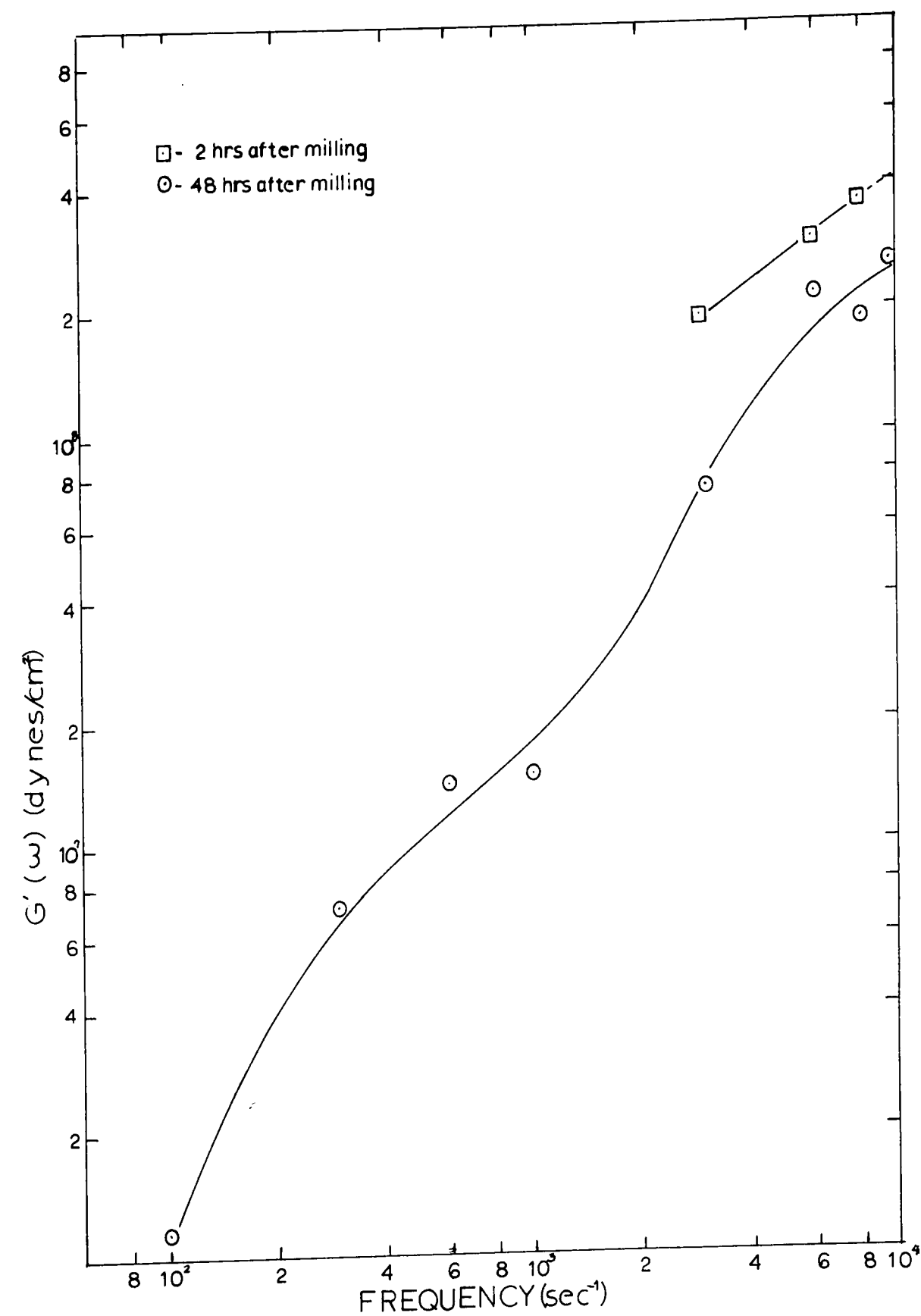


FIGURE 14- ELASTIC MODULUS VERSUS FREQUENCY
FOR 4% ELF 5 DISPERSION

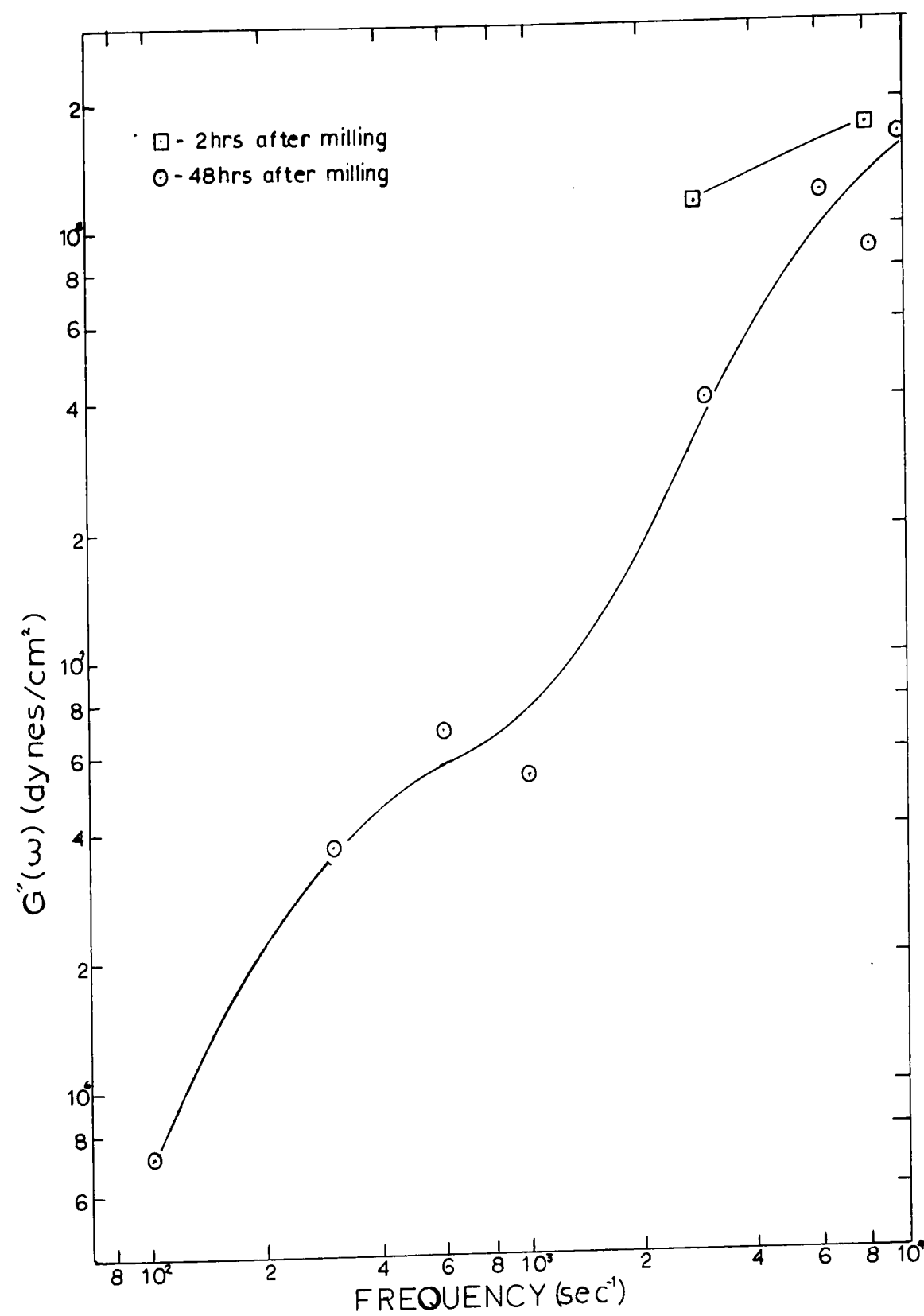


FIGURE 15- VISCOUS MODULUS VERSUS
FREQUENCY FOR 4% ELF5 DISPERSION

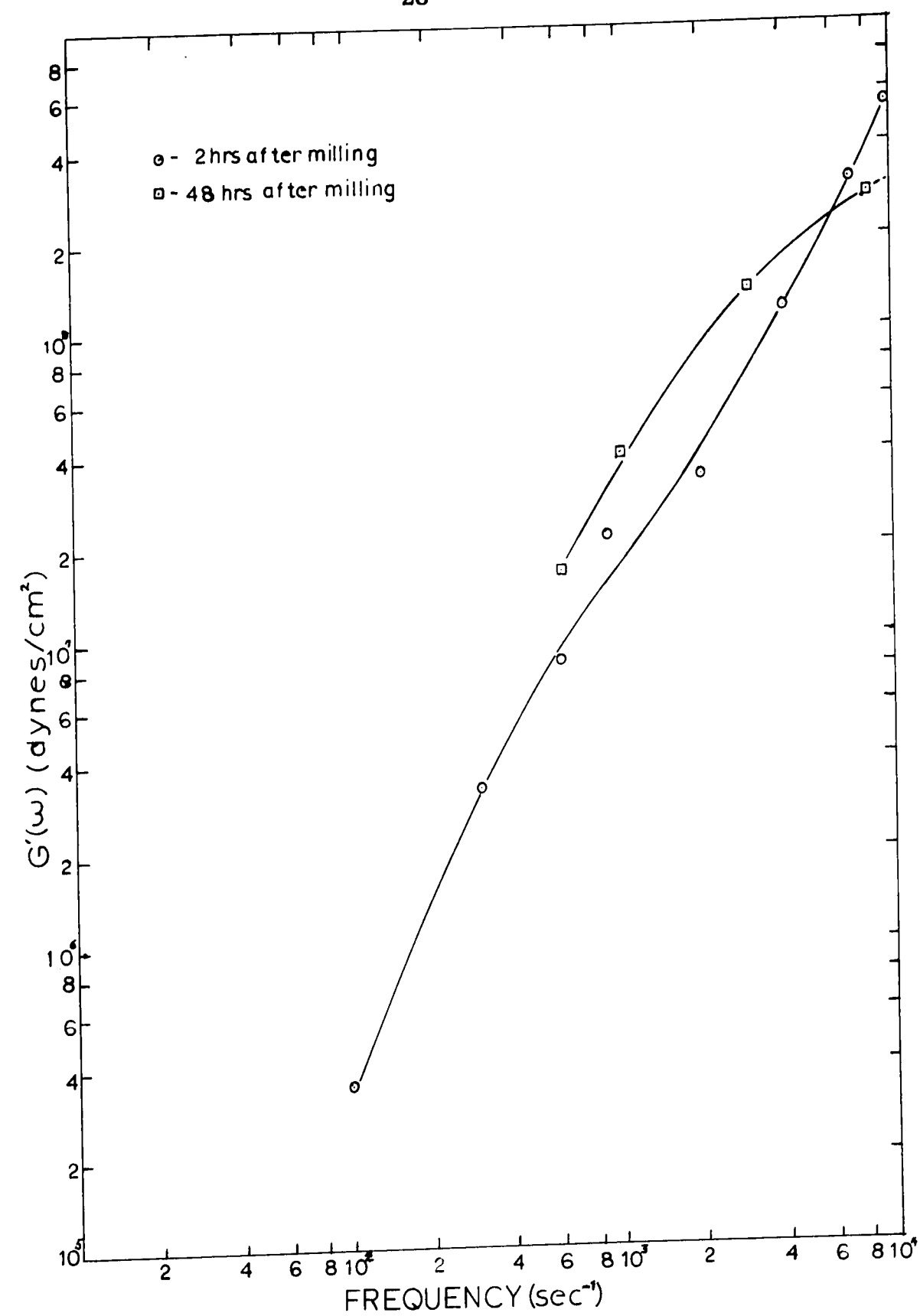


FIGURE 16-ELASTIC MODULUS VERSUS FREQUENCY
FOR 8% ELF5 DISPERSION

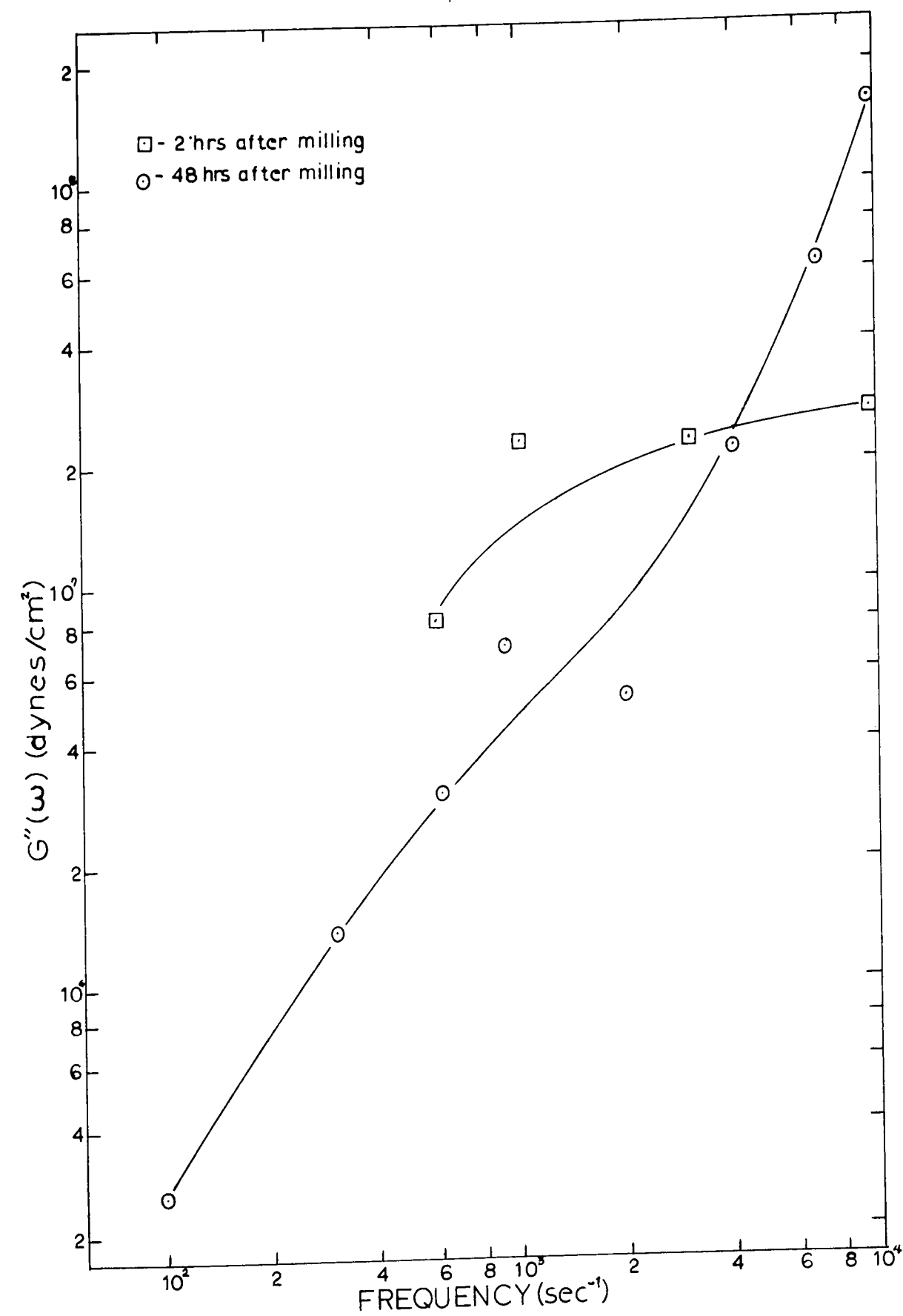


FIGURE 17- VISCOUS MODULUS VERSUS FREQUENCY
FOR 8% ELF 5 DISPERSION

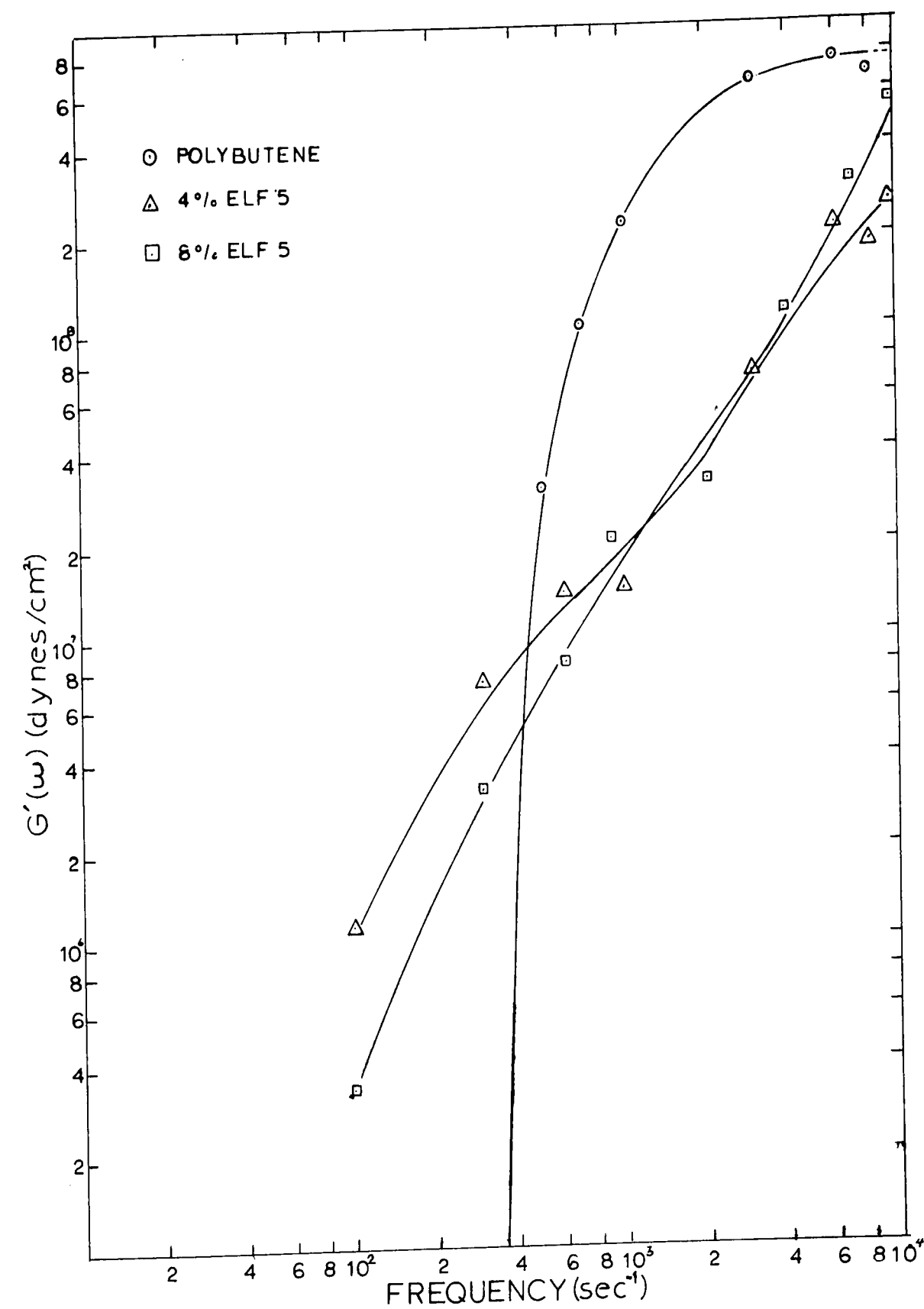


FIGURE 18- COMPARISON OF ELASTIC MODULUS
FOR SYSTEMS STUDIED

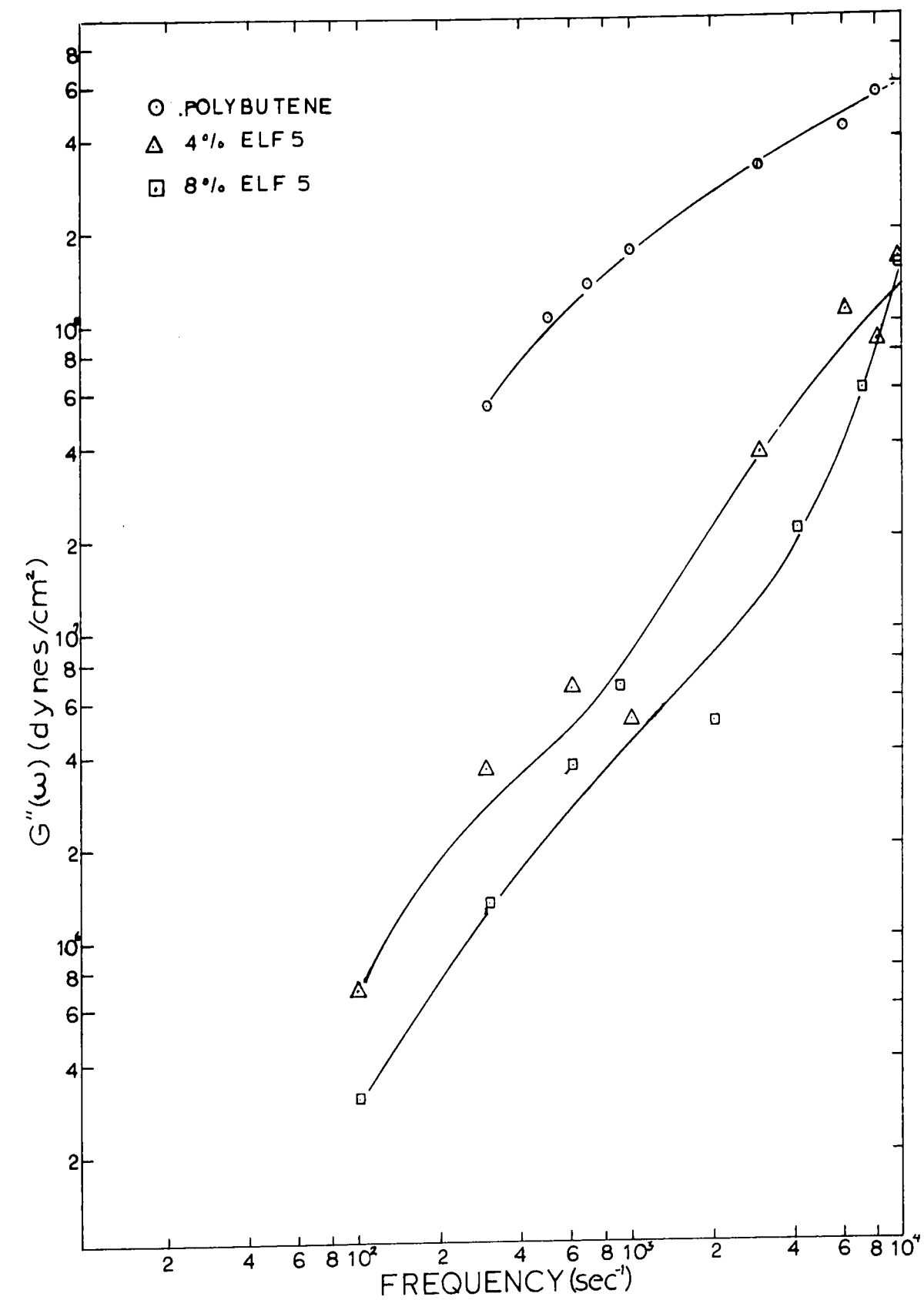


FIGURE 19 - COMPARISON OF VISCOUS MODULUS FOR SYSTEMS STUDIED

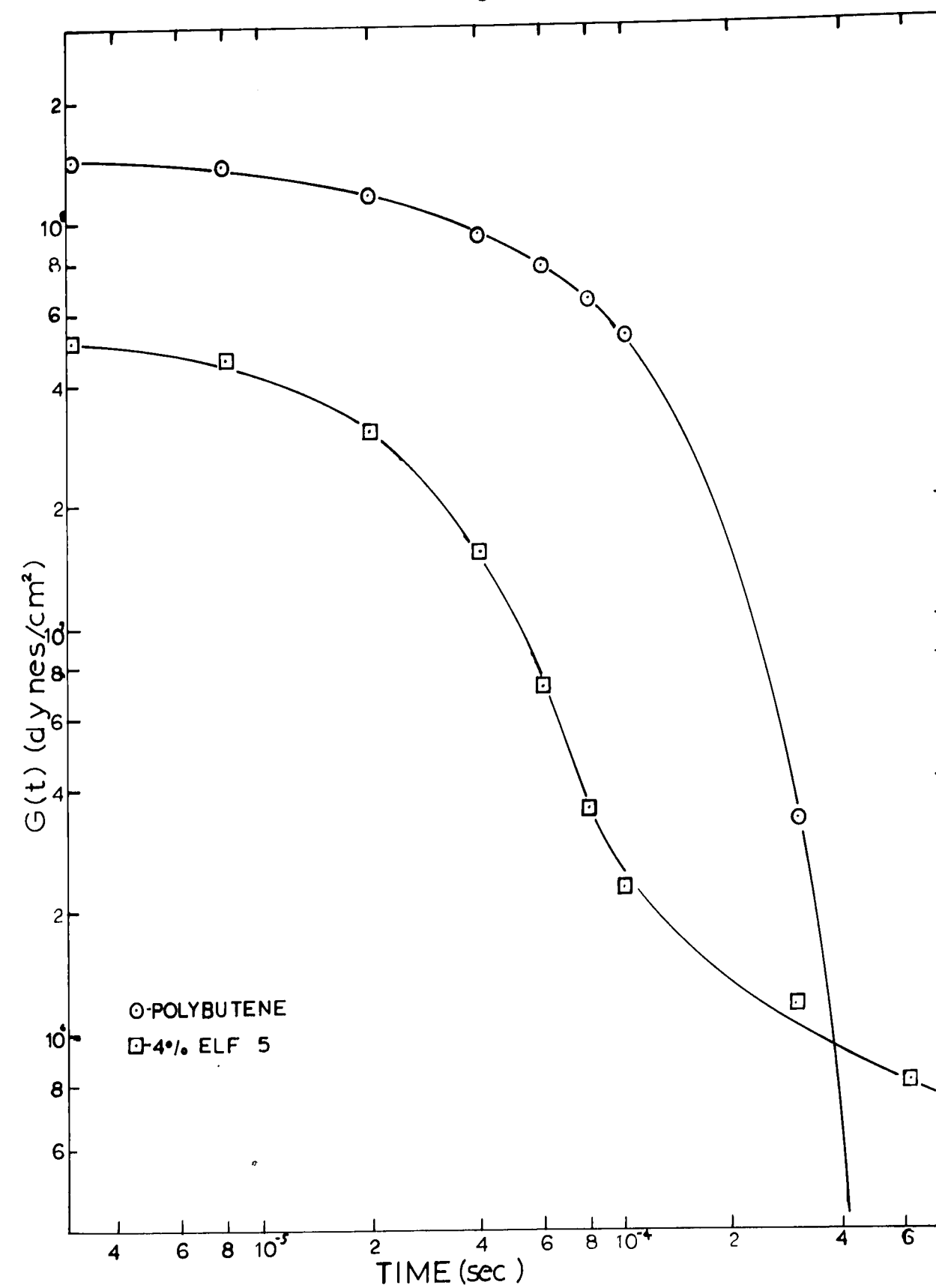


FIGURE 20-TIME DEPENDENT SHEAR MODULUS VERSUS TIME-POLYBUTENE AND 4% ELF 5 DISPERSION

were milled and again 48 hrs. after milling. Measurements at certain frequencies were obtained after 96 hrs. in the case of the 8% dispersion. Dispersions have been shown to set up(11) after milling and data was obtained at different times in an attempt to measure this phenomenon in terms of the shear modulus. Since the setting up occurs rapidly within the first 8 to 12 hrs. after milling, data had to be obtained within a 30 minute period if the results were to be meaningful. The entire frequency range could not be covered in this time, hence the data at 2 hrs. after milling was measured at only a few of the higher frequencies.

The shear modulus as from the data for pure H-50 is shown in Figures 12 and 13 and forms a smooth curve decaying with decreasing frequency. Ferry(1) shows that this is the expected shape of the curve for low molecular weight polymer.

The elastic components of the shear modulus for the dispersions fell more rapidly than that of the H-50 and was smaller in value at high frequencies. However, the values of the elastic component calculated for the 8% dispersion were greater than those of the 4% dispersion at high frequencies. One possible explanation for the shapes of the shear moduli curves is that in pure H-50 the molecules are entangled and closely associated so that at high rates of

strain a large elastic effect is present. The addition of carbon to the system contributes an elastic effect because of the carbon particle-particle structure which can occur in a dispersion. The elastic effect caused by the dispersion structure would be less than that of the H-50 for small deformations at high rates of strain. If the carbon particles limit the entanglement of the polymer molecules, it will cause the elastic effect in a dispersion to be smaller than that of the pure H-50 explaining the higher values of $G'(\omega)$ for pure H-50 with respect to dispersions at high rates of strain. Similar results have been obtained for the case of a polymer dissolved in a viscous solvent(12).

As more carbon black is added, the elastic effect of the carbon particle-particle structure would increase, explaining why $G'(\omega)$ for the 8% dispersion is larger than that of the 4% dispersion.

At low frequencies $G'(\omega)$ for both dispersions was larger than that of the pure H-50. One explanation is that at lower rates of strain, the pure H-50 is primarily viscous in behavior and the elastic effects of the carbon particle-particle structure would dominate the elastic modulus causing it to be larger than that of the H-50.

The viscous component of the shear modulus decreases

considerably with time after milling indicating that the dispersion is setting up. At high frequencies the viscous component of the 8% dispersion increased with time. This phenomenon is unexplained.

Values of $G'(\omega)$ and $G''(\omega)$ calculated from data measured for the 8% dispersion 96 hrs. after milling were not significantly different from those calculated after 48 hrs. indicating that set up occurs almost completely within 48 hrs. from time of milling.

The time-domain shear modulus, $G(t)$, was calculated using Equation 4 for pure H-50 and the 4% dispersion, and is shown in Figure 19. The values of $G'(\omega)$ for $\omega \rightarrow \infty$ were obtained by an extrapolation of the curves in Figures 12 and 14. The values used were 8.45×10^8 dynes/cm for the H-50 and 3.0×10^8 dynes/cm for the 4% dispersion. $G(t)$ was not calculated for the 8% dispersion since an extrapolation of Figure 15 could not be made with any degree of assurance that the correct value would be obtained. Relaxation times were calculated for the case of a fluid exhibiting simple exponential decay, i.e. $G(t) = G(0)\exp(-t/\theta)$. The values of θ obtained were 4.2×10^{-5} sec. for H-50 and 2.8×10^{-5} sec. for the 4% dispersion. These values are of the order of magnitude expected for thin viscoelastic fluids.

A comparison was made between the viscous modulus as calculated on the shearometer and the viscosity as determined by a rotational cup and bob viscometer to obtain an independent check on the accuracy of the shearometer. The comparison made use of the fact that $G''(\omega)/2\pi f = \eta'$, η' being the dynamic viscosity. The dynamic viscosity approaches the ordinary viscosity, η , as f becomes small. A linear extrapolation of the curve $\log \eta'$ versus $\log f$ was made to $\log f = 0$, as shown in Figure 21 and yielded a value of $\eta' = 150$ poise at $f = 1 \text{ sec}^{-1}$. The value of η as determined on the rotational viscometer was 190 poise. The two values agree within the experimental accuracy of the shearometer. Because of the length of the extrapolation (two decades of frequency) the accuracy of the extrapolation is questionable and lower frequency data is needed for definite comparison.

The first of two possible sources of error investigated is that the motion of the pick-up plate must be of such a magnitude that the motion-voltage relationship of the crystal is linear. Confirmation was obtained by plotting voltage input to the driver, which bears a linear relationship to the strain, against voltage output from the crystal. The points thus obtained plotted as a straight line shown in Figure 22. Linear viscoelastic behavior is also indicated

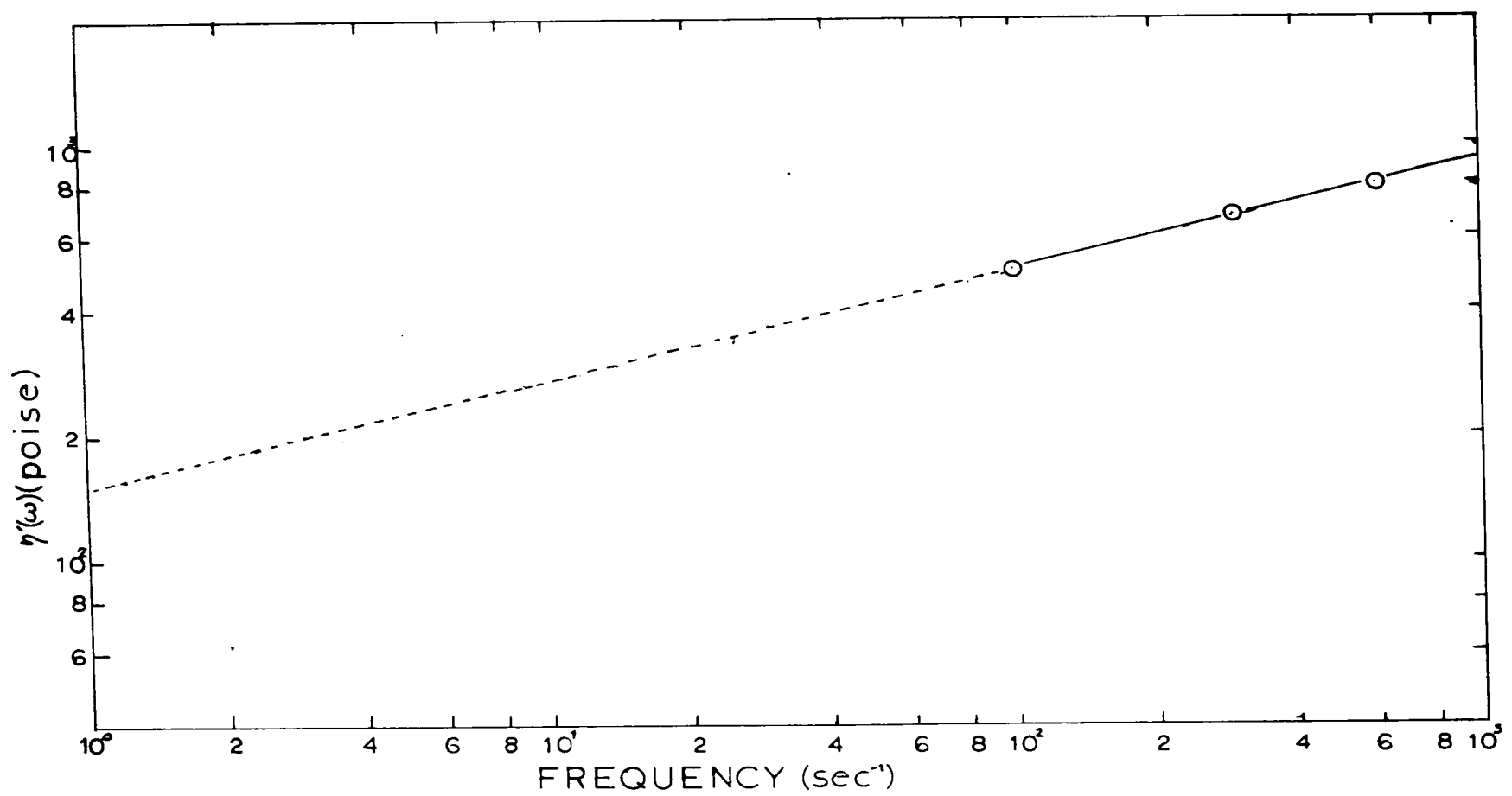


FIGURE 21- DYNAMIC VISCOSITY VERSUS FREQUENCY-
8% ELF 5 DISPERSION

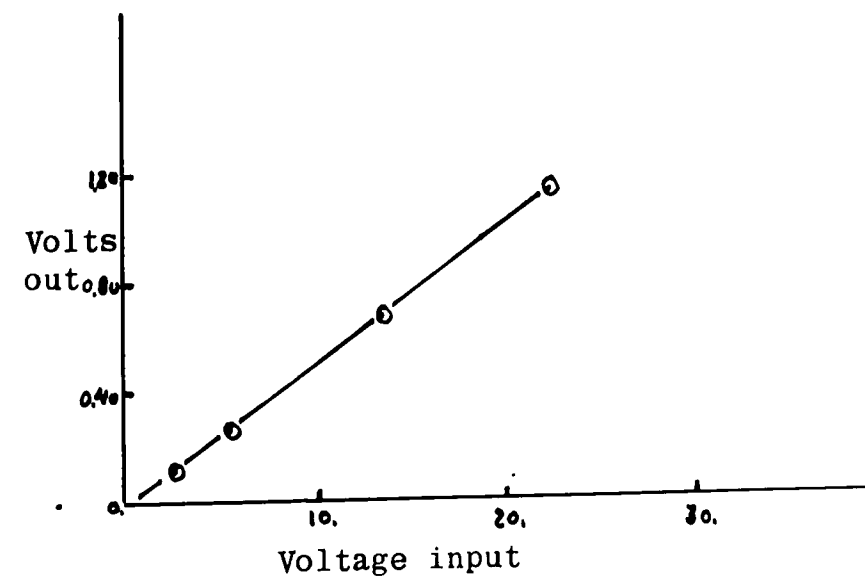


Figure 22-Linear response of transducer.

by this curve.

The second possible source of error is that the mass of the pick-up plate may cause a change of phase angle in the signal from the crystal. The phase change must be constant for the range of motion of crystal or the wave length measurement will be in error. Several different input voltages were introduced at a given frequency causing different amplitudes of motion of the pick-up plate. No change in phase angle was detected indicating that any change caused by the plate mass is constant over the range of motion experienced in this work. A more detailed analysis of force and motion at the pick-up plate will have to be completed in order to elucidate this effect.

Conclusions

The shearometer provides an accurate and feasible means for determining the shear modulus of a visco-elastic fluid by utilizing the theory developed by Ferry(1) but extending his experimental techniques to include opaque as well as transparent fluids. The addition of auxilliary components to replace the oscilloscope will provide ease of operation and allow rapid determination of the shear modulus for the fluid of interest. In principle the shearometer can be used over a wider range of frequency and viscosity than were reported here. Small modifications in the design of the instrument will greatly increase its range of operation.

The shearometer described here will measure wave lengths and critical damping factors of viscoelastic fluids over the frequency range, 100cps to 10Kc. The measurement of wave lengths and damping can be made with an experimental accuracy of 5 to 20%. The larger errors occurred at low frequencies where wave lengths are large and damping is small. Reproducibility of the data is also within 5 to 20%. The shear modulus calculated from the wave length and critical damping factor has an error of 10 to 65%.

There are some limitations to the method employed here for measuring the shear modulus. If the wave length to

damping factor ratio is too large, it may be difficult to measure the stress at the plate separations required to obtain a measurable phase angle shift.

The amplitude of motion of the driver plate must be small enough so that the viscoelastic behavior is linear.

There is a lower limit to the viscosity of the fluid being tested which is determined by whether the fluid will transmit a measurable signal. No work has been done to discover this limit.

Some limitations also exist which are functions of the design of the instrument rather than the method.

The viscosity of the fluids being tested has an upper limit. This upper limit is approximately 200 poise. At higher viscosities the fluid will not flow smoothly around the plates as they are being separated and a cantilever effect is experienced by the plates. This force will distort the output signal from the crystal.

Initial tests indicate that the upper limit of frequency is 10Kc. Above this frequency the driver response falls off very rapidly and it is not possible to obtain data above this frequency. The response of the pick-up transducer is also questionable above 10Kc.

The present method of taking data (photographs of

the oscilloscope traces) is costly and time consuming. Also measurements taken from these pictures are a major source of error in the data.

The pick-up transducer is extremely sensitive to external vibrations. Local 30cps vibrations were experienced in the work reported here caused by machinery in the immediate vicinity of the shearometer.

Recommendations For Future Work

1) The possibility of replacing the driver and the pick-up transducer with elements having a wider frequency should be explored. Use of two or more drivers, each covering a portion of the desired range, may be necessary. At frequencies above 20Kc, a piezoelectric driver may be practical

2) Redesign the plate mountings so that high viscosity materials can be studied. One possible design is to incorporate a mounting which will enable the pick-up plate to rotate 90°, so that as the plates are being separated the fluid will act on the plate edge rather than the face. When the desired separation is achieved the plate can be rotated back to its normal position, i.e. parallel to the driver.

3) Explore possibilities of replacing the oscilloscope with a phase angle meter and a high-sensitivity voltmeter. Information on a voltmeter is available in Appendix C. No information could be obtained on a low frequency phase angle meter except that it is not a common item.

4) The shearometer should be mounted on a vibration free surface.

Appendix AEquipment Specifications

Driver-Mustang M-12 Speaker; Frequency response, 35 to 10000cps;

Power handling capacity, 30 watts IPM; Price, \$18.90

Pick-up Transducer- Astatic No. 12 Phono-cartridge; Output

voltage, 4.0 volts; Price, \$4.70

Signal Generator-Hewlett-Packard 3300A Function Generator;

50 watts, Frequency range, 0.01cps to 100Kc;

Price, \$590.

Oscilloscope- Tektronix Type 502A Dual Beam Oscilloscope;

Sensitivity to 0.1 millivolt/cm; sweep rates to

1 usec/cm.

Dovetail Slide with Vernier- Tropel Inc, Fairmont, N.Y.,

Type A4515DE; Vernier reads 0.001 in.

Price, \$143.00

FIGURE 23-CIRCUIT DIAGRAM- RC AMPLIFIER

KEY:

T-Power transformer, 325-325 V, 70 ma; 5 v, 3 a; 6.3 v, 3.5 a.

S-Switch

F-Fuse, 1 a.

P-Plugs for jacks

Capacitors

C1-20 uf electrolytic, 45 v.

C2-50 uf

C3-0.27 uf

Resistors

R1-50 ohm, 10 w.

R2-8200 ohm, 2 w.

R3-1500 ohm

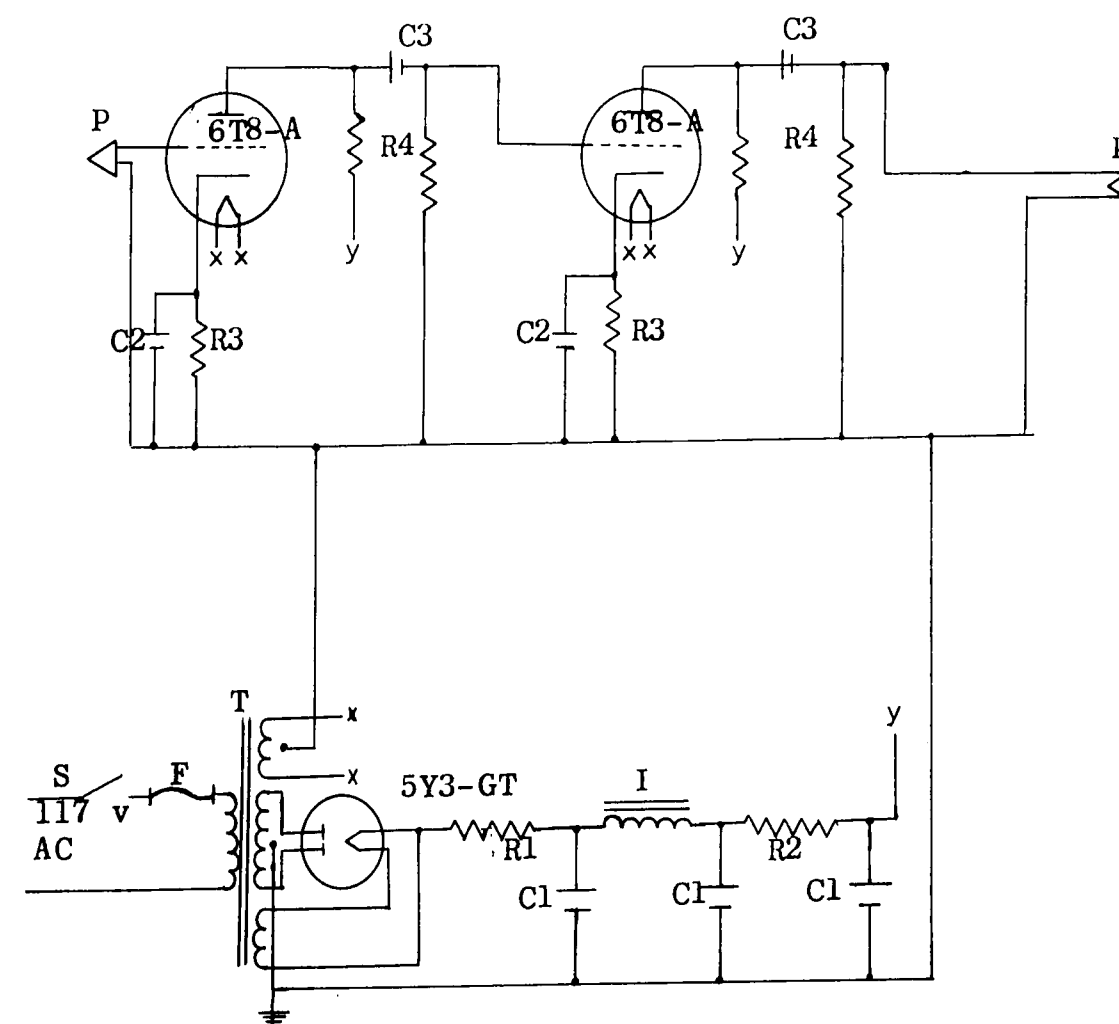
R4-0.1 megaohm

Tubes

6T8-A triode (RCA)

5Y3-GT full wave rectifier (RCA)

I-Inductor, filter choke



Appendix BData

H-50 Polybutene

Frequency (sec ⁻¹)	Wave length (in.)	Damping factor (in.)	G'(ω) (dynes/cm ²)	G''(ω) (x10 ⁶)
8K	1.8	0.65	675.	560.
6K	2.27	1.10	765.	426
3K	4.17	2.05	660.	324.
1K	7.78	2.20	222.	175.
700	10.0	2.37	104.	134.
500	12.4	2.54	33.	106.
300	16.5	2.65	0.	53.8

4% Elf-5 Dispersion(2 hrs after milling)

Frequency (sec ⁻¹)	Wave length (in.)	Damping factor (in.)	G'(ω) (dynes/cm ²)	G''(ω) (x10 ⁶)
8K	0.78	2.1	360.	-
6K	2.80	0.46	286.	166.
3K	6.25	0.32	203.	135.

4% Elf-5 Dispersion(48 hrs. after milling)

10K	0.77	0.35	254.	159.
8K	0.75	0.41	186.	85.4
6K	1.11	0.56	214.	109.
3K	1.30	0.64	73.5	38.3
1K	1.64	1.01	14.7	5.2
600	2.95	1.40	14.3	6.7
300	4.01	2.00	7.1	3.6
100	5.06	2.20	1.1	0.7

8% Elf-5 Dispersion (2 hrs. after milling)

Frequency (sec ⁻¹)	Wave length (in.)	Damping factor (in.)	G'(ω) (dynes/cm ²)	G''(ω) (x10 ⁶)
10K	0.54	0.61	---	26.2
8K	0.65	1.29	272.	
3K	1.56	1.43	133.	22.2
1K	2.56	2.11	38.5	22.8
600	3.4	1.35	16.6	8.

8% Elf-5 Dispersion(48 hrs. after milling)

10K	1.0	0.70	540.	152.
7K	1.02	0.75	298.	60.
4K	1.09	0.96	116.	21.
2K	1.14	1.16	32.7	5.
900	2.26	1.19	21.2	6.8
600	2.32	0.95	8.4	3.7
300	2.86	1.21	3.23	1.3
100	3.90	1.03	0.35	0.32

8% Elf-5 Dispersion(96 hrs. after milling)

8K	1.09	0.65	406.	
3K	1.30	0.95	87.	
600	2.35	1.16	9.4	

Appendix CMicro-Voltmeter

A new AC micro-voltmeter has been developed by Hewlett-Packard which may be acceptable for use with the shearometer as a replacement for measuring voltages from the oscilloscope. The voltmeter is capable of measuring 3 u volt to 3 volt signals over a 5 cps to 600 Kc range. The voltmeter will separate a desired signal from external noise if a reference signal of the frequency to be measured is available. The signal generator will provide this signal in the case of the shearometer. Accuracy is $\pm 3\%$ up to 60 Kc. The model number is 3410A and the list price is \$800.

References

- 1) Ferry, John D., Viscoelastic Properties of Polymers, John Wiley and Sons, New York.
- 2) Sittel, K; Rouse, P.E; and Bailey, E.D., Method for Determining the Viscoelastic Properties of Dilute Polymer Solutions at Audio-Frequencies, Journal of Applied Physics, Vol. 25 No 10, 1314, Oct. 1954.
- 3) Simmons, J.M., A Servo-controlled Rheometer for Measurement of the Dynamic Modulus of Viscoelastic Liquids, Journal of Scientific Instruments, Vol. 43, 887, Mar. 1966
- 4) Smith, T.L.; Ferry, J.D. and Schremp, F.W., Measurement of the Mechanical Properties of Polymer Solutions by Electromagnetic Transducers, Journal of Applied Physics, Vol. 40, 144, Feb. 1949.
- 5) Miles, D.O.; Sinusoidal Shear Generator for Study of Viscoelasticity, Journal of Applied Physics, Vol. 33, No. 4, 1422, Apr. 1962.
- 6) Miller, H.E., Jurgens, J.L. and Plunkett, R.; Measurement of Complex Shear Modulus of Thin Viscoelastic Layers, Technical Report TR-65-4, University of Minnesota, Institute of Technology, Oct. 1965.
- 7) Adler, F.T., Sawyer, W.M. and Ferry, J.D., Propagation of Transverse Waves in Viscoelastic Media, Journal of Applied Physics, Vol. 20, 1036, Nov. 1949.
- 8) Newman, S., A Vibrating Reed Apparatus for Measuring the Dynamic Mechanical Properties of Polymers, Journal of Applied Polymer Science, Vol. II, No. 6, 333, 1959.
- 9) ASTM Standard D-1316-54T, Fineness of Grind of Printing Ink by the Production Grindometer, 1954.
- 10) Fischhoff, G.M., Masters Research, Lehigh University, Bethlehem, Pa., 1967.
- 11) Navidad, R.B., Masters Research, Lehigh University, Bethlehem, Pa., 1966.

- 12) Philippoff, W., Dynamic Investigations of Polymer
Solutions in an Extended Range of Frequency,
Transactions of the Society of Rheology, Vol.
VIII, 117, 1964

Vita

Name: Richard Arnold Eelman

Place of Birth: Paterson, N.J.

Date of Birth: 28 April 1940

Parents: Harry and Edna C. Eelman

Education: Lehigh University, Bethlehem, Pa.

Degree: B.S. in Chemical Engineering, 1961, Lehigh University

Professional Experience: Plastics Engineer, ACF Industries
Inc., Albuquerque, N.Mex., 1961 to 1964.

First Lieutenant, U.S. Army, 1962 to 1965.

Present Employer: Chevron Oil Company, Perth Amboy, N.J.